Nonquenched Isoscalar Spin-*M*1 Excitations in *sd*-Shell Nuclei

H. Matsubara,[1,†] A. Tamii,[1] H. Nakada,[2] T. Adachi,[1] J. Carter,[3] M. Dozono,[5,‡] H. Fujita,[1] K. Fujita,[1,§] Y. Fujita,[1] K. Hatanaka,[1] W. Horiuchi,[6] M. Itoh,[7] T. Kawabata,[4,∥] S. Kuroita,[5] Y. Maeda,[9] P. Navrátil,[10] P. von Neumann-Cosel,[11] R. Neveling,[12] H. Okamura,[1,*] L. Popescu,[13,¶] I. Poltoratska,[11] A. Richter,[11] B. Rubio,[14] H. Sakaguchi,[1] S. Sakaguchi,[4,§] Y. Sakemi,[7] Y. Sasamoto,[4] Y. Shimbara,[15,**] Y. Shimizu,[4,††] F. D. Smit,[12] K. Suda,[1,††] Y. Tameshige,[1,‡‡] H. Tokieda,[4] Y. Yamada,[5] M. Yosoi,[1] and J. Zenihiro[8,††]

[1]Research Center for Nuclear Physics (RCNP), Osaka University, Ibaraki, Osaka 567-0047, Japan
[2]Department of Physics, Chiba University, Inage, Chiba 263-8522, Japan
[3]School of Physics, University of the Witwatersrand, Johannesburg 2050, South Africa
[4]Center for Nuclear Study (CNS), University of Tokyo, Bunkyo, Tokyo 113-0033, Japan
[5]Department of Physics, Kyushu University, Fukuoka 812-8581, Japan
[6]Department of Physics, Hokkaido University, Sapporo 060-0810, Japan
[7]Cyclotron and Radioisotope Center (CYRIC), Tohoku University, Sendai, Miyagi 980-8578, Japan
[8]Department of Physics, Kyoto University, Kyoto 606-8502, Japan
[9]Department of Applied Physics, Miyazaki University, Miyazaki 889-2192, Japan
[10]TRIUMF, 4004 Wesbrook Mall, Vancouver, British Columbia V6T 2A3, Canada
[11]Institut für Kernphysik, Technische Universität Darmstadt, D-64289 Darmstadt, Germany
[12]iThemba LABS, National Research Foundation, Somerset West 7129, South Africa
[13]Vakgroep Subatomaire en Stralingsfysica, Universiteit Gent, B-9000 Gent, Belgium
[14]Instituto of Fisica Corpuscular, CSIC-University de Valencia, E-46071 Valencia, Spain
[15]Graduate School of Science and Technology, Niigata University, Niigata 950-2102, Japan

(Received 25 December 2014; revised manuscript received 15 June 2015; published 1 September 2015)

Differential cross sections of isoscalar and isovector spin-$M1$ ($0^+ \to 1^+$) transitions are measured using high-energy-resolution proton inelastic scattering at $E_p = 295$ MeV on ^{24}Mg, ^{28}Si, ^{32}S, and ^{36}Ar at 0°–14°. The squared spin-$M1$ nuclear transition matrix elements are deduced from the measured differential cross sections by applying empirically determined unit cross sections based on the assumption of isospin symmetry. The ratios of the squared nuclear matrix elements accumulated up to $E_x = 16$ MeV compared to a shell-model prediction are 1.01(9) for isoscalar and 0.61(6) for isovector spin-$M1$ transitions, respectively. Thus, no quenching is observed for isoscalar spin-$M1$ transitions, while the matrix elements for isovector spin-$M1$ transitions are quenched by an amount comparable with the analogous Gamow-Teller transitions on those target nuclei.

DOI: 10.1103/PhysRevLett.115.102501 PACS numbers: 25.40.Ep, 21.10.Hw, 27.30.+t

Spin-isospin responses in nuclei play an important role in nuclear physics and astrophysics [1–3]. One of the fundamental modes is of the type $\Delta J^\pi = 1^+$ that corresponds to Gamow-Teller (GT: $\Delta T_z = \pm 1$) and magnetic-dipole ($M1$: $\Delta T_z = 0$) transitions. The relevant transition rates are often taken from shell-model predictions. Experimental transition strengths are, however, found to be quenched when compared to the theoretical predictions using bare operators and are reproduced only by introducing effective operators. Quenching is a basic property of nuclear structure and influences astrophysical processes as well. The nuclear spin responses and their quenching have strong effects on the mean free path of neutrinos in dense neutron matter, on the dynamics and neutrino nucleosynthesis in core-collapse supernovae [4], and the cooling of proto-neutron stars [5,6]. Furthermore, exhaustion of a sum rule of the spin strengths is relevant to the spin susceptibility of asymmetric nuclear matter [7] and its response to the strong magnetic field in magnetars [8].

The quenching phenomenon has been extensively studied for spin-flip transitions of the GT type. The GT quenching is explained mainly by the mixing with higher-order configurations primarily resulting from the tensor interaction [9,10]. The $M1$ operator provides another case of a spin-flip transition. It consists of spin and orbital angular-momentum terms which can be of isoscalar (IS: $\Delta T = 0$) and isovector (IV: $\Delta T = 1$) nature. The IV spin-$M1$ operator mediates transitions that are analogues to GT under the assumption of isospin symmetry. IV spin-$M1$ transitions are, thus, expected to be quenched similarly as GT transitions [11]. Various theoretical studies [12–15] suggest that the quenching of IS spin-$M1$ transitions in *sd*-shell nuclei is similar to that of the IV ones. Experimental information on IS spin-$M1$ transitions is, however, scarce leading to large uncertainties with respect to a possible quenching.

The spin-$M1$ operator is common among the strong, electromagnetic, and weak interaction. For studying IS spin-$M1$ quenching, the (p, p') reaction is a superior probe compared with the (e, e') [16] or (γ, γ') [17] reactions because of its selectivity solely to spin-$M1$ excitations due to the local nature of the nucleon-nucleon (NN) interaction [18]. Previous experimental studies using the (p, p') reaction indicated that the quenching of IS spin-$M1$ transitions was stronger than that of the IV ones [19] and that IV transitions often exhibited no quenching [20] inconsistent with the observed quenching at analog GT transitions. It was not clear to what extent these controversial results were caused by limitations with respect to the sensitivity of the J^π assignments of excited states or by the model for the conversion from the differential cross sections to strengths.

This Letter reports on new high-energy-resolution (p, p') scattering data and the extracted IS and IV spin-$M1$ quenching factors obtained by a comparison with $0\hbar\omega$ shell-model calculations. The new data show significant improvements when compared to the former work [19,20]. (i) High energy-resolution (p, p') measurements at extremely forward scattering angles including 0° [21] have greatly enhanced the signal-to-noise ratio. (ii) Only even-even self-conjugate nuclei were selected as targets. This allows an unambiguous distinction of IS and IV spin-$M1$ transitions. (iii) The unit cross section, which is the conversion factor from the observed differential cross sections to the squared nuclear matrix element (SNME), has been obtained from experimental data.

The experiments were performed at the Research Center for Nuclear Physics (RCNP), Osaka University. A proton beam at $E_p = 295$ MeV was transported to the west-south (WS) beam line [22]. Dispersion matching [23] between the beam line and the Grand Raiden (GR) spectrometer [24] was realized to achieve an energy resolution of 18 keV (FWHM). Protons inelastically scattered from the target to angles from 0° to 14° were momentum analyzed by the GR spectrometer with two sets of multiwire drift chambers and two plastic scintillation counters. A detailed description of the experimental techniques can be found in Ref. [21].

Self-supporting foils of ^{24}Mg, ^{28}Si, and ^{32}Si were used as targets. The ^{32}Si target was kept at the liquid nitrogen temperature in order to prevent sublimation by charged particle irradiation [25]. A gas-target system with aramid window foils [26] was employed for ^{36}Ar.

An excitation energy spectrum of the ^{28}Si(p, p') reaction at scattering angles 0°–0.5° is shown in Fig. 1(a). Excited states below $E_x = 16$ MeV are well separated from each other. The angular distribution of the differential cross sections of each state was compared to distorted-wave impulse approximation (DWIA) calculations for identifying the $0^+ \to 1^+$ transitions. The DWIA calculations were performed with the code DWBA07 [27] using one-body transition densities obtained from shell-model calculations with the code NuShellX@MSU [28] incorporating the USD interactions [12,29]. The effective NN interaction

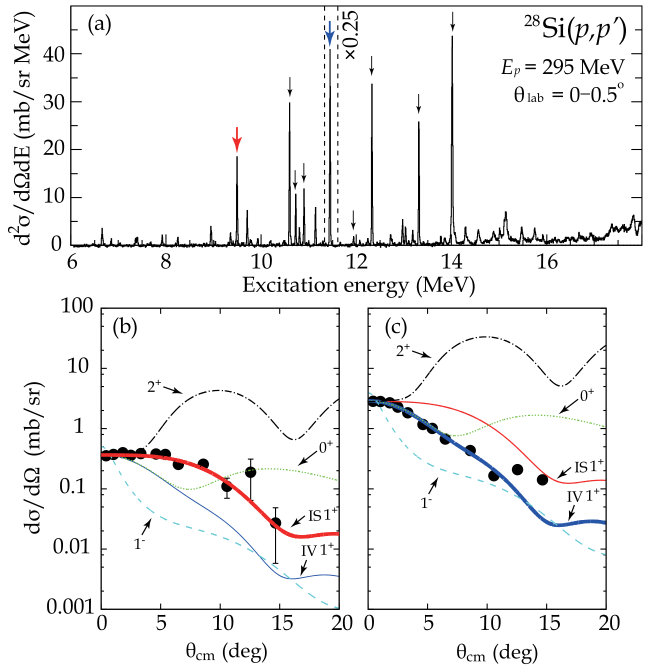

FIG. 1 (color online). (a) Excitation energy spectrum of the ^{28}Si(p, p') reaction at $E_p = 295$ MeV and $\theta_{\rm lab} = 0°$–$0.5°$. The arrows in the figure indicate states which are assigned definitely as 1^+. Angular distributions of (b) an IS and (c) an IV spin-$M1$ transition marked by red and blue arrows in (a), respectively, in comparison with theoretical angular distributions for several multipolarities.

of Love and Franey [30] at 325 MeV was used. Optical potential parameters were obtained from the elastic scattering data [31]. Oscillator parameters were taken from global parameters [32].

In Figs. 1(b) and 1(c), the angular distributions of the differential cross section for transitions to the states at $E_x = 9.495$ (1^+: $T = 0$) and 11.447 MeV (1^+: $T = 1$) in ^{28}Si are compared with DWIA calculations for several multipolarities ($J^\pi = 0^+$, 1^+, 1^-, and 2^+). The theoretical curves are normalized to the experimental data at the most forward angle. The angular distribution of the IS spin-$M1$ excitation is flatter than the IV one due to the contribution of an exchange tensor component in the effective NN interaction [30]. Thus, the shape of the angular distribution allows a clear isospin determination for each spin-$M1$ excitation. The resulting isospin assignments are in good agreement with those from (e, e') scattering [33–37] for $M1$ transitions seen in both experiments.

We identified 1–4 (4–8) states for each target nucleus to result from IS (IV) spin-$M1$ transitions (cf. Fig. 2). In addition, 1–3 (1–7) states were assigned as IS (IV) transitions to 1^+ states with less confidence indicated by the "+" label in Fig. 2. They are included in the estimation of experimental uncertainties. We reassigned between one and six states in each nucleus as 0^+ instead of 1^+ claimed in the previous work [19,20].

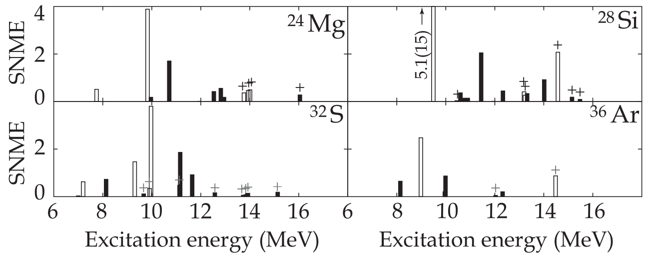

FIG. 2. Observed distributions of IS and IV-spin-$M1$ SNME [open (filled) bars represent IS (IV) transitions]. The bars labeled + indicate states with a less confident spin assignment.

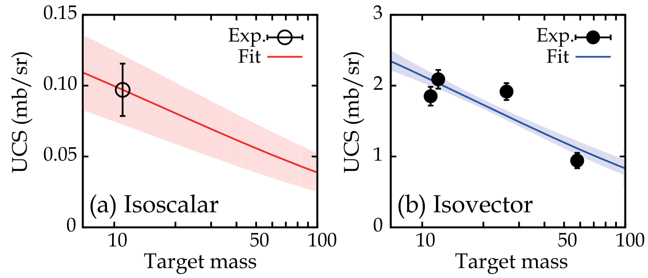

FIG. 3 (color online). Mass dependences of the UCS for (a) IS and (b) IV transitions.

The differential cross section at 0° is approximately proportional to the SNME. The IS and IV spin-$M1$ reduced nuclear matrix elements for transitions from the ground state $|\mathrm{g.s.}\rangle$ to an excited state $|f\rangle$ are defined by

$$M_f(\vec{\sigma}) = \frac{1}{\sqrt{2J_i+1}}\left\langle f \left\| \sum_{k=1}^{A} \vec{\sigma}_k \right\| \mathrm{g.s.} \right\rangle, \quad (1)$$

$$M_f(\vec{\sigma}\tau_z) = \frac{1}{\sqrt{2J_i+1}}\left\langle f \left\| \sum_{k=1}^{A} \vec{\sigma}_k \tau_{z,k} \right\| \mathrm{g.s.} \right\rangle, \quad (2)$$

respectively, where $\vec{\sigma}_k$ is the Pauli spin matrix, and $\tau_{z,k}$ is the z component of the isospin operator for the kth nucleon. The factor $1/\sqrt{2J_i+1}$ is unity for a 0^+ ground state. The unit cross section (UCS) is defined as the ratio of the differential cross section to the SNME at momentum transfer $q = 0$. We define a UCS ($\hat{\sigma}_{\mathrm{IS}}$ and $\hat{\sigma}_{\mathrm{IV}}$) for IS and IV spin-$M1$ transitions analogous to the GT strength [38]

$$\frac{d\sigma}{d\Omega}(0°) = \hat{\sigma}_T F_T(q, E_x)|M_f(\mathcal{O})|^2, \quad (3)$$

where the subscript T represents either IS or IV and $\mathcal{O}$ either the $\vec{\sigma}$ or $\vec{\sigma}\tau_z$ operator. Here, $F_T(q, E_x)$ is a kinematic factor which accounts for the finite momentum transfer (q) and excitation energy (E_x). It can be obtained from a DWIA calculation. The target mass dependence of the UCS can be parametrized as [38]

$$\hat{\sigma}_T(A) = N_T \exp(-xA^{1/3}), \quad (4)$$

where N_T and x are free parameters. The mass-dependent factor x essentially arises from distortion effects common to IS and IV transitions and, thus, is taken to be the same. DWIA calculations indicate this assumption remains better than 5%.

The parameters N_{IV} and x in Eq. (4) have been fitted to four experimentally obtained IV UCSs. The value $\hat{\sigma}_{\mathrm{IV}}$ has been derived from Eq. (3) using the (p, p') data and the IV spin-$M1$ SNME deduced from the GT SNME on the assumption of isospin symmetry. In addition, the GT SNME has been obtained from $(^3\mathrm{He}, t)$ measurements and β-decay lifetimes [39,40]. The factor N_{IS} has been calibrated using $^{11}\mathrm{B}(p, p')$ data [41] and an IS $M1$ strength deduced from the γ-decay lifetimes of the first excited mirror states in ^{11}B and ^{11}C [40]. Note that the linear combination of the γ-decay strengths is proportional to the IS SNME, owing to isospin symmetry. Details on the UCSs can be found in Ref. [31].

The results for the IS and IV UCSs are shown in Fig. 3, where the bands represent the fitting error. Note that the experimentally obtained IS (IV) UCS value is 50% lower (20% higher) than the theoretically obtained value used in the previous work [19,20].

Each differential cross section at 0° has been converted to the IS or IV spin-$M1$ SNME using Eq. (3), as shown in Fig. 2. The sums up to $E_x = 16$ MeV are plotted as a function of the target mass in Fig. 4. Here, shell-model calculations using the USD interaction [12] are shown as solid lines. (The difference between predictions of the summed $M1$ strength using the USD and the newer USDA and B [29] interactions is less than 10% and, thus, not significant in the following discussion.) The quenching factors defined as the ratio of the observed SNMEs to the theoretical predictions summed up to 16 MeV are 1.01(9) and 0.61(6) for the IS and the IV spin-$M1$ transitions,

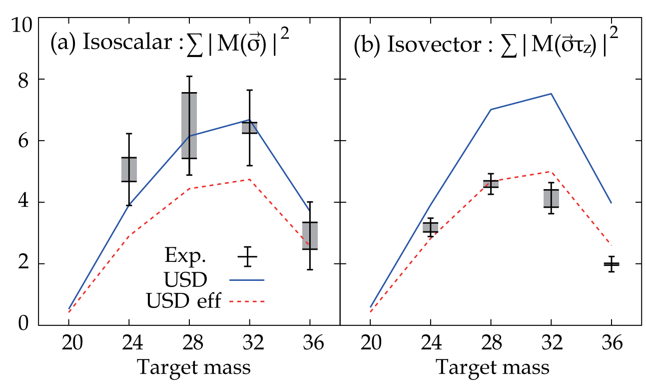

FIG. 4 (color online). Accumulated sums of the spin-$M1$ SNMEs for (a) IS and (b) IV transitions up to $E_x = 16$ MeV. The error bars and gray bands indicate the total experimental uncertainties and the partial uncertainties from the spin assignment, respectively. The solid lines and dotted lines are the predictions of shell-model calculations using the USD with bare and effective g factors, respectively.

respectively, where the factors are averaged over the nuclei measured. Note that the quenching factor of the IS spin-$M1$ transitions is close to unity, while that of the IV ones is significantly smaller and consistent with the study of analogous GT transitions [42]. The calculations with empirical effective g factors [12] are shown by dotted lines in Fig. 4 (USD eff). The SNMEs of the IV spin-$M1$ transitions are reproduced well by USD eff (χ^2/N values for the USD and USD eff predictions are 13 and 0.8, respectively, where N is the number of data points). In contrast, the IS transitions are better described by USD (χ^2/N values for USD and USD eff predictions are 0.5 and 2.2, respectively). The present result shows that the widely used effective g factors lead to an overquenching for IS spin-$M1$ transitions in the sd shell.

The effective IS g factor was determined to reproduce the diagonal spin matrix element $\langle S\rangle$ of the ground state; see Eq. (20) in Ref. [43]. Experimental $\langle S\rangle$ values were obtained from the IS magnetic moments of mirror nuclei and subtracting the contribution of the total angular momentum J. Although the quenching of $\langle S\rangle$ in nuclei of the closed LS shell plus or minus one nucleon was obvious [12–15], the quenching in the mid-sd-shell was insignificant [43]. The finding is consistent with our observation of no IS quenching of $M1$ transitions in the mid-sd-shell.

In order to shed some light on these observations, we next consider the difference $\Delta_{\rm spin}$ between the sums of the IS and IV spin-$M1$ SNMEs as a function of E_x,

$$\Delta_{\rm spin}(E_x) = \frac{1}{16}\left\{\sum_{E_f<E_x}|M_f(\vec{\sigma})|^2 - \sum_{E_f<E_x}|M_f(\vec{\sigma}\tau_z)|^2\right\}, \quad (5)$$

where the sum is taken up to E_x. With the total spin operators for protons (neutrons) $\vec{S}_{p(n)}(=\frac{1}{2}\sum_{i=1}^{Z(N)}\vec{\sigma}_{p(n),i})$, IS and IV spin-$M1$ transitions are represented by $\frac{1}{2}M_f(\vec{\sigma}) = \langle f|\vec{S}_p+\vec{S}_n|\text{g.s.}\rangle$ and $\frac{1}{2}M_f(\vec{\sigma}\tau_z) = \langle f|\vec{S}_p-\vec{S}_n|\text{g.s.}\rangle$, respectively. In the limit of $E_x\to\infty$, the completeness of $|f\rangle$ yields

$$\langle(\vec{S}_p+\vec{S}_n)^2\rangle = \sum_f \langle\text{g.s.}|\vec{S}_p+\vec{S}_n|f\rangle\langle f|\vec{S}_p+\vec{S}_n|\text{g.s.}\rangle$$
$$= \lim_{E_x\to\infty}\frac{1}{4}\sum_{E_f<E_x}|M_f(\vec{\sigma})|^2, \quad (6)$$

and $\langle(\vec{S}_p-\vec{S}_n)^2\rangle = \lim_{E_x\to\infty}\frac{1}{4}\sum_{E_f<E_x}|M_f(\vec{\sigma}\tau_z)|^2$. Here the expectation value is taken for the 0^+ ground state. We then derive

$$\lim_{E_x\to\infty}\Delta_{\rm spin}(E_x) = \langle\vec{S}_p\cdot\vec{S}_n\rangle, \quad (7)$$

which represents the spin correlation between protons and neutrons in the ground state.

Figure 5 shows experimental $\Delta_{\rm spin}(E_x)$ and theoretical $\langle\vec{S}_p\cdot\vec{S}_n\rangle$ values for nuclei in several shell regions. In

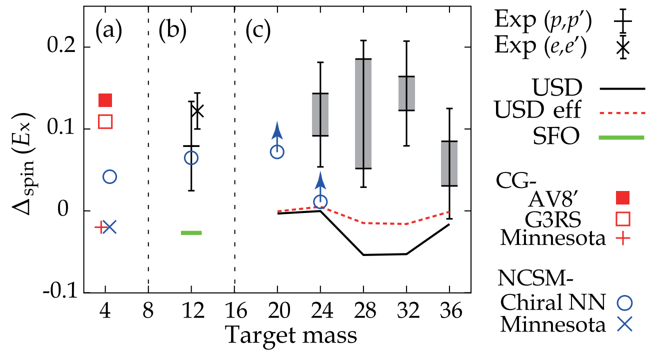

FIG. 5 (color online). Experimental $\Delta_{\rm spin}(E_x)$ and theoretical $\langle\vec{S}_p\cdot\vec{S}_n\rangle$ values explained in the text for (a) ^{4}He, (b) ^{12}C, and (c) sd-shell nuclei. The experimental results in (c) are summed up to $E_x = 16$ MeV with the same definition of the error bars as in Fig. 4. The arrows of the NCSM results in (c) indicate that the results are considered to represent a lower limit.

Fig. 5(a), $\langle\vec{S}_p\cdot\vec{S}_n\rangle$ values from state-of-the-art nuclear structure calculations for ^{4}He using the correlated Gaussian (CG) method [44] and no-core shell model (NCSM) [45] are displayed. Realistic (AV8' [46] and G3RS [47]) and chiral [48] NN forces give positive values due to the tensor correlation, in contrast to the Minnesota [49] interaction, which does not contain the tensor force. Figure 5(b) compares experimental results for $\Delta_{\rm spin}$ in ^{12}C derived from (p,p') [21] and (e,e') [50] experiments with $\langle\vec{S}_p\cdot\vec{S}_n\rangle$ values obtained from shell-model calculations. Both the experiments and the NCSM with realistic forces show positive values while a calculation using the effective Suzuki-Fujimoto-Otsuka interaction [51] gives a slightly negative value. Finally, Fig. 5(c) shows $\Delta_{\rm spin}$ values derived from the present data in comparison to the shell-model calculations using the USD interaction discussed above. Note that the strengths predicted in the latter are almost exhausted up to 16 MeV. The data show positive values as in ^{12}C and comparable to the values predicted with realistic forces for lower mass nuclei. In contrast, the shell-model calculations are unable to reproduce the experimental results irrespective of the use of bare or effective g factors or using other effective g factors [13–15].

However, predictions by the NCSM (open blue circles) indicate positive $\langle\vec{S}_p\cdot\vec{S}_n\rangle$ values for ^{20}Ne ($N_{\rm max}=4$) and ^{24}Mg ($N_{\rm max}=2$). Here, $N_{\rm max}$ defines the maximal allowed harmonic-oscillator excitation energy above the unperturbed ground state [45] and, hence, represents a measure of the model space. The results (−0.007, 0.028, and 0.072 for $N_{\rm max}=0$, 2, and 4 for ^{20}Ne and −0.018 and 0.011 for $N_{\rm max}=0$ and 2 for ^{24}Mg, respectively) show a clear correlation with the size of $N_{\rm max}$ but are considered to represent a lower boundary only because they have not yet converged for the present $N_{\rm max}$ values. The increase of $\langle\vec{S}_p\cdot\vec{S}_n\rangle$ with increasing $N_{\rm max}$ implies that mixing with higher-lying orbits due the tensor correlation is important for reproducing $\Delta_{\rm spin} > 0$ values. This should be verified in future NCSM calculations which might be possible up to $N_{\rm max} = 8$ for the nuclei under investigation [52]. It is remarkable to see the positive $\langle \vec{S}_p \cdot \vec{S}_n \rangle$ values hinted by the NCSM calculation as the experimental $\Delta_{\rm spin}(16~{\rm MeV})$ indicates, despite the limitation of the excitation energy. It would be interesting to study the IS and IV strength distributions at higher energy.

In summary, proton inelastic scattering at very forward angles has been measured on $N = Z$ *sd*-shell nuclei for the study of the IS and IV spin-$M1$ SNMEs. Systematically, no quenching of the IS spin-$M1$ SNMEs has been observed. The present result may provide new insights into the mechanism of the quenching of spin matrix elements in nuclei. The difference in the quenching between the IS and IV spin-$M1$ SNMEs may be attributed to the spin correlation between protons and neutrons in the ground state, which is closely connected to the concepts of spin-aligned *np* pairs [53], *np* pairing [54], and high-momentum correlated nucleon pairs [55] in nuclei.

We would like to thank M. Ichimura, H. Toki, Y. Ogawa, T. Myo, I. Tanihata, and B. A. Brown for valuable discussions. We are indebted to the RCNP cyclotron staff for providing us the excellent beam. This work was supported by the JSPS International Training Program (ITP) and was partially supported by JSPS (Grants No. 14740154, No. 24654066, No. and 25105509), by MICIN-Spain (Grant No. FPA2011-24553), by the JSPS-CSIC collaboration program, and by the DFG under Contracts No. SFB 634 and No. NE 679/3-1.

[*]Deceased.
[†]Present address: National Institute of Radiological Sciences (NIRS), Japan.
mats.hiroaki@gmail.com
[‡]Present address: CNS, University of Tokyo, Japan.
[§]Present address: Department of Physics, Kyushu University, Japan.
[∥]Present address: Department of Physics, Kyoto University, Japan.
[¶]Present address: SCK-CEN, Belgium.
[**]Present address: CYRIC, Tohoku University, Japan.
[††]Present address: RIKEN Nishina Center, Japan.
[‡‡]Present address: Fukui Prefectural Hospital, Japan.

[1] F. Osterfeld, Rev. Mod. Phys. **64**, 491 (1992).
[2] K. Langanke and G. Martinez-Pinedo, Rev. Mod. Phys. **75**, 819 (2003).
[3] K. Heyde, P. von Neumann-Cosel, and A. Richter, Rev. Mod. Phys. **82**, 2365 (2010).
[4] K. Langanke, G. Martinez-Pinedo, P. von Neumann-Cosel, and A. Richter, Phys. Rev. Lett. **93**, 202501 (2004); **100**, 011101 (2008).
[5] S. Reddy, M. Prakash, J. M. Lattimer, and J. A. Pons, Phys. Rev. C **59**, 2888 (1999).
[6] A. Burrows and R. F. Sawyer, Phys. Rev. C **58**, 554 (1998).
[7] S. Fantoni, A. Sarsa, and K. E. Schmidt, Phys. Rev. Lett. **87**, 181101 (2001); G. Shen, S. Gandolfi, S. Reddy, and J. Carlson, Phys. Rev. C **87**, 025802 (2013).
[8] A. Rabhi, M. A. Perez-Garcia, C. Providencia, and I. Vidana, Phys. Rev. C **91**, 045803 (2015).
[9] M. Ichimura, H. Sakai, and T. Wakasa, Prog. Part. Nucl. Phys. **56**, 446 (2006).
[10] G. F. Bertsch and I. Hamamoto, Phys. Rev. C **26**, 1323 (1982).
[11] P. von Neumann-Cosel, A. Poves, J. Retamosa, and A. Richter, Phys. Lett. B **443**, 1 (1998).
[12] B. A. Brown and B. H. Wildenthal, Nucl. Phys. **A474**, 290 (1987).
[13] I. S. Towner and F. C. Khanna, Nucl. Phys. **A399**, 334 (1983).
[14] I. S. Towner, Phys. Rep. **155**, 263 (1987).
[15] A. Arima, K. Shimizu, W. Bentz, and H. Hyuga, Adv. Nucl. Phys. **18**, 1 (1987).
[16] A. Richter, Nucl. Phys. **A374**, 177c (1982).
[17] U. E. P. Berg, K. Ackermann, K. Bangert, C. Bläsing, W. Naatz, R. Stock, K. Wienhard, M. K. Brussel, T. E. Chapuran, and B. H. Wildenthal, Phys. Lett. **140B**, 191 (1984).
[18] F. Petrovitch, and W. G. Love, Nucl. Phys. **A354**, 499c (1981).
[19] N. Anantaraman, B. A. Brown, G. M. Crawley, A. Galonsky, C. Djalali, N. Marty, M. Morlet, A. Willis, J.-C. Jourdain, and B. H. Wildenthal, Phys. Rev. Lett. **52**, 1409 (1984).
[20] G. M. Crawley, C. Djalali, N. Marty, M. Morlet, A. Willis, N. Anantaraman, B. A. Brown, and A. Galonsky, Phys. Rev. C **39**, 311 (1989).
[21] A. Tamii *et al.*, Nucl. Instrum. Methods Phys. Res., Sect. A **605**, 326 (2009).
[22] T. Wakasa *et al.*, Nucl. Instrum. Methods Phys. Res., Sect. A **482**, 79 (2002).
[23] Y. Fujita, K. Hatanaka, G. P. A. Berg, K. Hosono, N. Matsuoka, S. Morinobu, T. Noro, M. Sato, K. Tamura, and H. Ueno, Nucl. Instrum. Methods Phys. Res., Sect. B **126**, 274 (1997); H. Fujita *et al.*, Nucl. Instrum. Methods Phys. Res., Sect. A **484**, 17 (2002).
[24] M. Fujiwara *et al.*, Nucl. Instrum. Methods Phys. Res., Sect. A **422**, 484 (1999).
[25] H. Matsubara, H. Sakaguchi, T. Kishi, and A. Tamii, Nucl. Instrum. Methods Phys. Res., Sect. B **267**, 3682 (2009).
[26] H. Matsubara, A. Tamii, Y. Shimizu, K. Suda, Y. Tameshige, and J. Zenihiro, Nucl. Instrum. Methods Phys. Res., Sect. A **678**, 122 (2012).
[27] J. Raynal, computer code DWBA07, Report No. NEA-1209/008.
[28] B. A. Brown and W. D. M. Rae, Nucl. Data Sheets **120**, 115 (2014).
[29] B. A. Brown and W. A. Richter, Phys. Rev. C **74**, 034315 (2006); W. A. Richter, S. Mkhize, and B. A. Brown, Phys. Rev. C **78**, 064302 (2008).
[30] M. A. Franey and W. G. Love, Phys. Rev. C **31**, 488 (1985).
[31] H. Matsubara, Ph.D. thesis, Osaka University, 2010; H. Matsubara *et al.* (to be published).
[32] M. W. Kirson, Nucl. Phys. **A781**, 350 (2007).

[33] W. L. Bendel, L. W. Fagg, S. K. Numrich, E. C. Jones, and H. F. Kaiser, Phys. Rev. C **3**, 1821 (1971).
[34] A. Richter, A. Weiss, O. Hausser, and B. A. Brown, Phys. Rev. Lett. **65**, 2519 (1990).
[35] C. Lüttge, P. von Neumann-Cosel, F. Neumeyer, C. Rangacharyulu, A. Richter, G. Schrieder, E. Spamer, D. I. Sober, S. K. Matthews, and B. A. Brown, Phys. Rev. C **53**, 127 (1996).
[36] F. Hofmann, P. von Neumann-Cosel, F. Neumeyer, C. Rangacharyulu, B. Reitz, A. Richter, G. Schrieder, D. I. Sober, L. W. Fagg, and B. A. Brown, Phys. Rev. C **65**, 024311 (2002).
[37] C. W. Foltz, D. I. Sober, L. W. Fagg, H. D. Gräf, A. Richter, E. Spamer, and B. Alex Brown, Phys. Rev. C **49**, 1359 (1994).
[38] T. N. Taddeucci, C. A. Goulding, T. A. Carey, R. C. Byrd, C. D. Goodman, C. Gaarde, J. Larsen, D. Horen, J. Rapaport, and E. Sugarbaker, Nucl. Phys. **A469**, 125 (1987); M. Sasano *et al.*, Phys. Rev. C **79**, 024602 (2009).
[39] Y. Fujita, B. Rubio, and W. Gelletly, Prog. Part. Nucl. Phys. **66**, 549 (2011), and references therein.
[40] R. B. Firestone *et al.*, *Table of Isotopes*, 8th ed. (John Wiley & Sons, New York, 1996).
[41] T. Kawabata *et al.*, Phys. Rev. C **70**, 034318 (2004).
[42] B. D. Anderson, T. Chittrakarn, A. R. Baldwin, C. Lebo, R. Madey, P. C. Tandy, J. W. Watson, C. C. Foster, B. A. Brown, and B. H. Wildenthal, Phys. Rev. C **36**, 2195 (1987); **43**, 50 (1991).
[43] B. A. Brown and B. H. Wildenthal, Phys. Rev. C **28**, 2397 (1983).
[44] Y. Suzuki, W. Horiuchi, M. Orabi, and K. Arai, Few-Body Syst. **42**, 33 (2008).
[45] B. R. Barrett, P. Navrátil, and J. P. Vary, Prog. Part. Nucl. Phys. **69**, 131 (2013).
[46] B. S. Pudliner, V. R. Pandharipande, J. Carlson, S. C. Pieper, and R. B. Wiringa, Phys. Rev. C **56**, 1720 (1997).
[47] R. Tamagaki, Prog. Theor. Phys. **39**, 91 (1968).
[48] D. R. Entem and R. Machleidt, Phys. Rev. C **68**, 041001 (2003).
[49] R. Thompson, M. Lemere, and Y. C. Tang, Nucl. Phys. **A286**, 53 (1977).
[50] P. von Neumann-Cosel, H.-D. Gräf, U. Krämer, A. Richter, and E. Spamer, Nucl. Phys. **A669**, 3 (2000).
[51] T. Suzuki, R. Fujimoto, and T. Otsuka, Phys. Rev. C **67**, 044302 (2003).
[52] R. Roth (private communication).
[53] B. Cederwall *et al.*, Nature (London) **469**, 68 (2011).
[54] S. Frauendorf and A. O. Macchiavelli, Prog. Part. Nucl. Phys. **78**, 24 (2014).
[55] R. Subedi *et al.*, Science **320**, 1476 (2008).